

# Study on Strengthening Slab - Column Connection with CFRP in a Flat Slab

Vishnu M.K<sup>1</sup>, Laju Kottalil<sup>2</sup>

<sup>1</sup>P.G Student, Mar Athanasius Collage of Engineering, kothamangalam, Kerala, India

<sup>2</sup>Professor, Dept. of Civil Engineering, Mar Athanasius College of Engineering Kothamangalam, Kerala, India

\*\*\*

**Abstract** -Retrofitting of slab-column connections has become a crucial concern as they are highly vulnerable to fail in punching shear failure. External strengthening is practically feasible rather than the post-installation of shear reinforcement in deteriorated slab column connections. In this paper, finite element analysis (FEA) is performed in order to investigate the punching shear strength of medium scale slab-column junctions strengthened with seven different alternative arrangements of Carbon Fiber Reinforced Polymer (CFRP) was studied and also studying the effectiveness of CFRP on high strength concrete and low strength concrete with comparing punching shear strength of models. The results indicated that the skewed placement of CFRP at the shear critical area is effective than that of orthogonal placement in the presence of end anchorage. Using CFRP sheet, in addition to steel reinforcing bars as flexural reinforcement improves the punching shear strength of slabs. This improvement can be significant for the slabs made of high strength concrete and low steel reinforcement ratio

**Key Words:** Flat slab, Punching shear Strengthening, FEA, CFRP

## 1. INTRODUCTION

Flat slab is reinforced concrete slab supported directly by concrete columns without the use of beams. Flat slab is defined as one sided or two sided support systems with shear load of the slab being concentrated on the supporting columns. Flat slab are considered suitable for most of the construction and for asymmetric column layouts like floors with curved shapes and ramps etc. The advantages of applying flat slabs are many like solution, flat soffit and flexibility in design layout. Even though building flat slabs can be an expensive affair but gives immense freedom to architects and engineers the luxury of designing. Punching shear is a type of failure of reinforced concrete slabs subjected to high localized forces. In flat slab structures this occurs at column support points.

### 1.1 Punching shear failure

Punching shear is a type of failure of reinforced concrete slabs subjected to high localized forces. This type of failure is catastrophic because no visible signs are shown prior to failure. A typical flat plate punching shear failure is characterized by the slab failing at the intersection point of the column. This results in the column breaking through the

portion of the surrounding slab. This type of failure is one of the most critical problems to consider when determining the thickness of flat plates at the column-slab intersection. Accurate prediction of punching shear strength is a major concern and absolutely necessary for engineers so they can design a safe structure.

Conventional wisdom does not apply when considering the mechanism of a punching shear failure; in a slab system with a concentrated load or at a slab column connection, the loaded area is not actually pushed through the slab. Punching shear failures arise from the formation of diagonal tension cracks around the loaded area, which result in a conical failure surface.

### 1.2 Flat slab strengthening techniques

The most important lesson is that an adequate inspection and a subsequently strengthening intervention would have avoided such collapses. To meet this new demand for repairing existing buildings, several techniques have been developed.

Massimo Lapia et al.[9] investigated Strengthening techniques against punching of R/C flat slabs could be grouped into four types: shear strengthening, flexural strengthening, enlargement of the support and post-tensioning systems. Shear strengthening represents one of the first strengthening technique against punching investigated by the researchers, it is performed through the installation of steel bolts or other shear reinforcements. Flexural strengthening consists in gluing external FRP strips on the top of the slab. Lot of researching are done on this field the CFRP act as a dowel action with addition of flexural steel reinforcement against to punching shear. The enlargement of the support may be obtained through the insertion of concrete or steel capital or widening the column section. Concerning the last strengthening technique, which uses post-tensioning systems, it represents a general technique to strengthen R/C structural elements.

In this paper, some numerical studies have been conducted to propose methods for strengthening of flat slabs with FRP sheets against punching failure. It has been shown that a simple and effective method for strengthening of slabs against punching failure is to use FRP sheets as flexural reinforcement. According to the previous studies Birkle G et al, 2008 and BS 8110 Code [5], flexural reinforcing bars increase the punching shear strength. By applying FRP

sheets on the tension side of slabs, the flexural strength of slabs and thus the punching shear strength is expected to increase.

## 2. FINITE ELEMENT MODELING

With the advances in modern computing techniques. Finite element analysis has become a practical and powerful tool for engineering analysis and design. In structural engineering, development of structural design code equations or redeveloping them is continues process and requires a wide range of experimental studies The problem gets enormously simplified with the use of ABAQUS 6.14 [2]

The main objective is to find out the failure and corresponding deflection and crack pattern of each flat slab and comparing the results.

Modelling of concrete and steel was done using 3D solid continuum 6-node linear triangular prism elements with reduced integration (C3D6R), CFRP was modelled using 6-node triangular in-plane shell elements (SC6R) and the adhesive layer was modelled using 6- node three-dimensional cohesive element (COH3D6). Rigid body modelled using linear quadrilateral elements of type (R3D4) and linear triangular elements of type (R3D3)

By considering the symmetry of a panel, one-quarter of each specimen was modeled with relevant boundary conditions as shown in Fig. 1 [9]. The symmetric planes were restrained in their perpendicular directions the bottom part of the slab was restrained in the vertical direction using constraints in the FEM analysis Fig. 1 The analysis type performed was quasi-static ABAQUS/Explicit because it performs faster than ABAQUS/Standard. Though it uses dynamic solution procedures for calculations, under slow loading rates it gives approximate static solutions [4]. Further, it has been assumed that, the actual load applied to the column transfers the load evenly as a pressure onto the slab area where the column was situated.

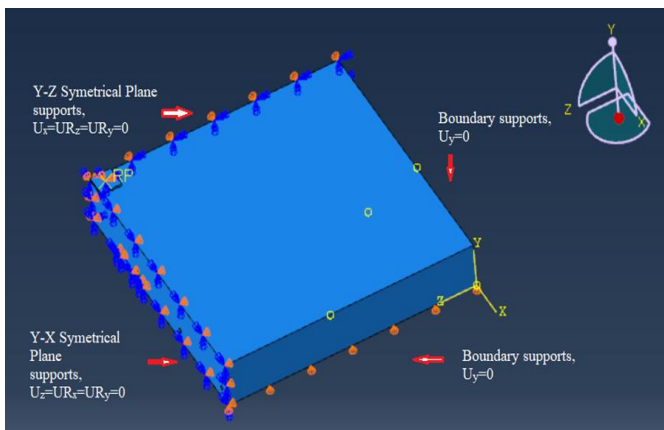


Fig-1: boundary condition and loading of the specimen

The Quasi-Static analysis in ABAQUS/Explicit performed by introducing velocity through the column stub till failure. The Quasi-Static analysis in ABAQUS/Explicit in good agreement with the experimental results as speculated by Genikomso [4]

The velocity was increasing with a smooth amplitude curve from 0(mm/s) to 100 (mm/s). The Fig. 1 shows the model, boundary condition and loading of the specimen.

### 2.1 Concrete damaged plasticity model in ABAQUS

The nonlinear behaviour of concrete is attributed to the process of damage and plasticity. The process of damage can be attributed to micro cracking, coalescence, and decohesion, etc. The plasticity behaviour can be characterized by several phenomenon such as strain softening, progressive deterioration, and volumetric expansion, etc. These lead to the reduction of the strength and stiffness of concrete, damage is usually characterized by the degradation of stiffness

### 2.2 Material modeling

The concrete material parameters that were used in the presented analyses are: the modulus of elasticity  $E_0$ , the Poisson's ratio  $\nu$  and the compressive and tensile strengths of the selected slabs. The concrete damaged plasticity model considers a constant value for the Poisson's ratio,  $\nu$ , even for cracked concrete The uniaxial stress-strain response of concrete in tension is linear elastic up to its tensile strength,  $f'_t$ . After cracking, the descending branch is modelled by a softening process, which ends at a tensile strain  $\epsilon_u$ , where zero residual (Fig.2)

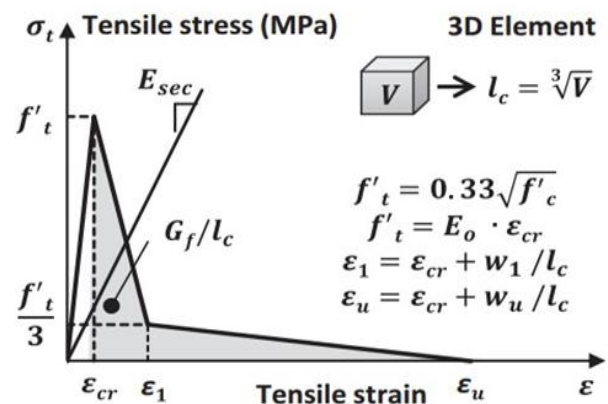


Fig-2: Uniaxial tensile stress-strain relationship for concrete.

The concrete's brittle behaviour is often characterized by a stress-crack displacement response instead of a stress-strain relationship. The stress-crack displacement relationship can be defined with different options: linear, bilinear or exponential tension softening response. Bilinear stiffening response was used and was calculated according to the Fig. 3

Where,  $f'_t$  is the maximum tensile strength and  $G_f$  denotes the fracture energy of concrete that represents the area under the tensile stress-crack displacement curve.

The fracture energy  $G_f$  depends on the concrete quality and aggregate size and can be obtained from Eq. (1)

$$G_f = G_{f0} \left( \frac{f_{cm}}{f_{cm0}} \right)^{0.7} \quad 1$$

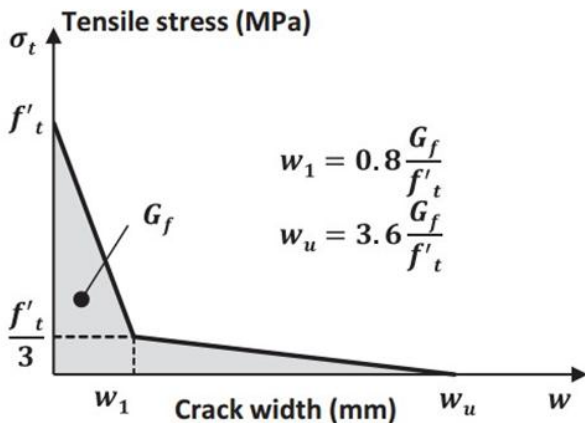


Fig -3: Uniaxial tensile stress–crack width relationship for concrete

Where  $f_{cm0} = 10$  MPa and  $G_f(f_0)$  is the base fracture energy depending on the maximum aggregate size,  $d_{max}$ . The value of the base fracture energy  $G_f(f_0)$  is 0.026 N/mm for maximum aggregate size  $d_{max}$ . Equal to 10 mm that was used in the tested specimens. The,  $f_{cm}$  is the mean compressive strength of concrete and its relationship with the characteristic value,  $f_{ck}$  is:  $f_{cm} = f_{ck} + 8$  MPa. In order to minimize the localization of the fracture, the tensile strains were used and they were defined by dividing the cracking displacement ( $w$ ) by the characteristic length of the element ( $l_c$ ). For 3D elements the characteristic length can be defined as the cubic root of the element's volume. The adopted critical length ( $l_c$ ) in the following simulations was 20 mm. The tensile stress–strain graph is illustrated in Fig.2

Concrete in compression was modeled with the Hognestad parabola (Fig.4). The assumed stress–strain relation behavior of the concrete under uniaxial compressive loading can be divided into three domains. The first one represents the linear-elastic branch, with the initial modulus of elasticity,  $E_0 = 5500\sqrt{f'c}$ . The linear branch ends at the stress level of  $\sigma_{co}$  that here is taken as:  $\sigma_{co} = 0.4 f'c$ . The second section describes the ascending branch of the uniaxial stress–strain relationship for compression loading to the peak load at the corresponding strain level,  $\epsilon_0 = (2f'c)/E_{sec}$ . The secant modulus of elasticity is defined as:  $E_{sec} = 5000\sqrt{f'c}$ . The third part of the stress–strain curve after the peak stress and until the ultimate strain  $\epsilon_u$  represents the post-peak branch. The equation for the assumed compressive stress–strain diagram is given in Fig.4

Damage was introduced in concrete damaged plasticity modeling tension and compression according to Fig. 5. And Fig.6, respectively. Concrete damage was assumed to occur in the softening range in both tension and compression. In compression the damage was introduced after reaching the peak load corresponding to the strain level  $\epsilon_0$ . Quite often material test data are supplied using values of nominal stress and strain, in such situations, the expressions presented below to convert the plastic material data from nominal data from nominal stress/strain values must use.

The classical metal plasticity model in ABAQUS defines the post - yield behaviour for most metal. It is possible to use a very close approximation of the actual material behaviour. The plastic data define the true yield stress of the material as a function of true plastic strain. The first piece of data given defines the initial yield stress of the material and, therefore should have a plastic strain value of zero.

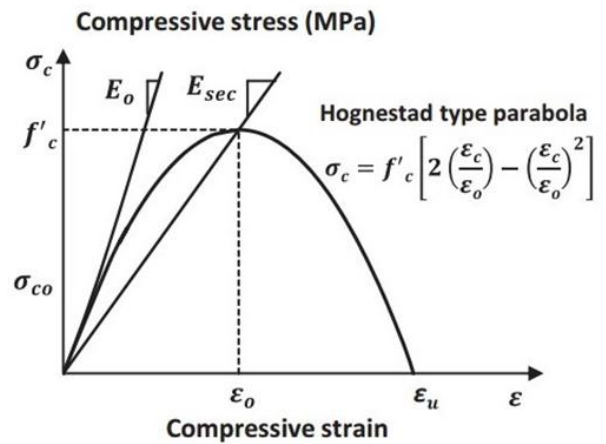


Fig. 4. Uniaxial compressive stress–strain relationship for concrete

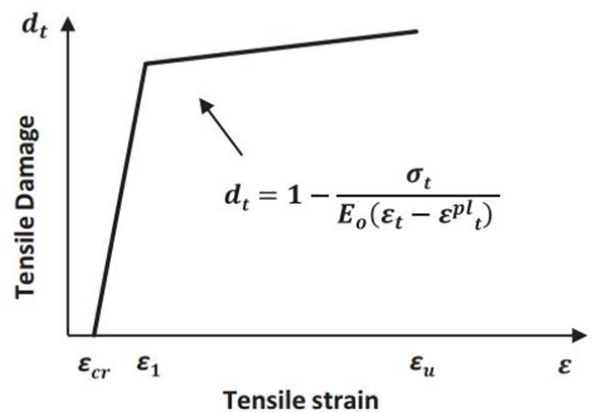


Fig.5. Tensile damage parameter–strain relationship for concrete.

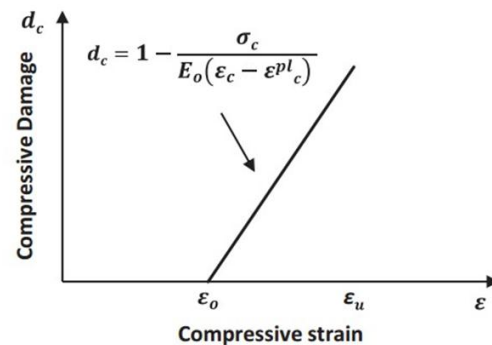


Fig. 6. Compressive damage parameter–strain relationship for concrete.

The strains provided in material. Instead, they will probably be the total strains in the material. The plastic strain obtained by subtracting the elastic strain, defined as the value of true stress divided by the young's modulus, from the value of total strain, Fig 7

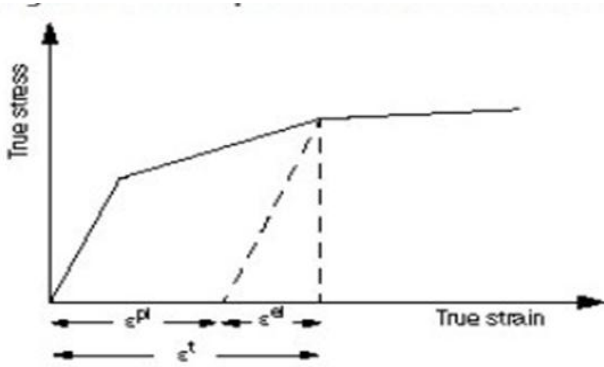


Fig.7 Decomposition of total strain into elastic and plastic components.

### 3. VALIDATION

The specimen model was prepared in the ABAQUS 6.14. With given property to each material as per Silva et.al. (2019)[9]. the slab column connection were externally strengthened using CFRP strip as shown in Fig.8

The CFRP size as 1 mm x 100 mm x 700 mm, and the concrete's measured 28th day average compressive strength was 28 N/mm<sup>2</sup> with a standard deviation of 3.38 N/mm<sup>2</sup>. The yield strength of steel was 500 N/mm<sup>2</sup> and the nominal cover to the steel reinforcements was 20 mm. The typical reinforcement detail of a sample is shown in Fig.9

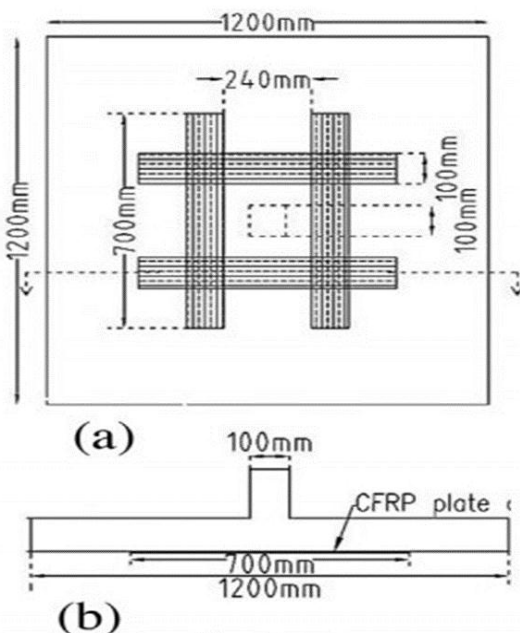


Fig.8. CFRP attached on tension face in orthogonal direction with end anchorage

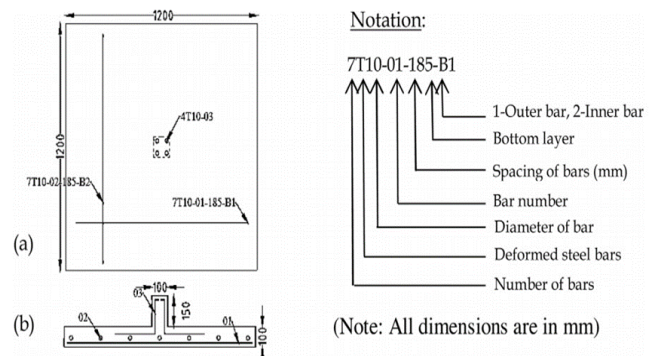


Fig.9. Reinforcement Details, (a) Plan, (b) Sectional elevation

During the test, simply supports were applied at the location of the line of contra flexure which is simulated in ABAQUS by applying vertical restraints at the perspective location[9]. Details regarding the material properties, reinforcement and test results are presented in Table1 and Fig 8 shows that schematic diagram of the test slab.

Table -1: Material properties and test results of specimen

property	value
Compressive Strength of Concrete, $f_c$ (MPa)	28
Tensile Strength of Concrete, $f_t$ (MPa)	1.75
Yield Strength of Steel Reinforcement, $f_y$ (MPa)	500
Area of Tensile reinforcement, $A_{st}$ (mm <sup>2</sup> )	100
Tensile reinforcement $P_s$ (%)	0.55
Yield Strength of CFRP, (MPa)	4000
Yield Strength of Epoxy, (MPa)	45
Failure load, (KN)	130
Displacement at failure (mm)	11.2

The failure load and displacement predicted by the simulation and the test are presented in Table 2

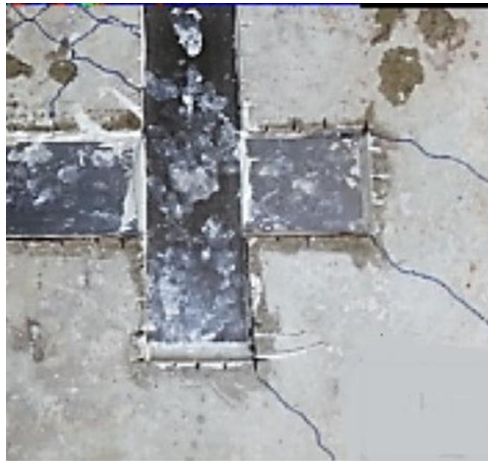
Table -2: Comparison between tested and FE model results

Specimen	Failure Load (kN)	Displacement at Failure (mm)
Test a	137.34	11.6
Test b	122.63	10.69
Isolated FEA	144.7352	9.769

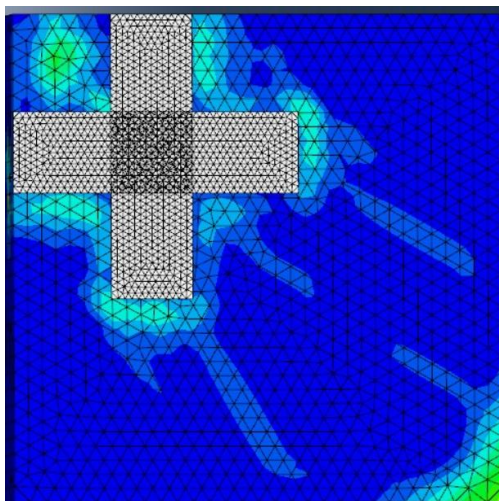
The FEA and experiment are in good agreement and both gives brittle punching shear failure. 6.66 % The FE model shows stiffer response than the test specimen. This can be attributed to the formation of initial crack developed at the tension surface of the specimen at the ultimate load.

By comparing the crack pattern between the FE models. Fig.4.5 (b) and the test specimen Fig.10 (a), it is obvious that in the test. From the observation made in the failure pattern of the slab. Brittle failure followed the formation of punching

shear cone. In the FE model crack pattern using simple supports. Fig.10 (b) shows strain concentrations near the slab edges. The punching shear formation in FE model and test specimen are in good agreement.



(a) Tested specimen



(b) FE Model

**Fig.10** Crack Pattern on Tension Surface at Ultimate Load

It is clear from the above Table 2 and crack propagation pattern, crack pattern of the isolated flat slab obtained from FEA is found to be in good agreement with experimental results. The trend line of load displacement graph obtained from experimental results and analytical study follow similar path. The failure load and displacement obtained by both methods are within acceptable limits. The crack pattern are also found to be similar.

#### 4. MODELLING OF STRENGTHENED FLAT SLAB MODELS

By considering specimens symmetry. One quarter of the strengthened flat slab models used for simulation. The material properties and arrangements reinforcement of previously validated model used in other model. Fig.11 shows schematic diagram of strengthening schemes

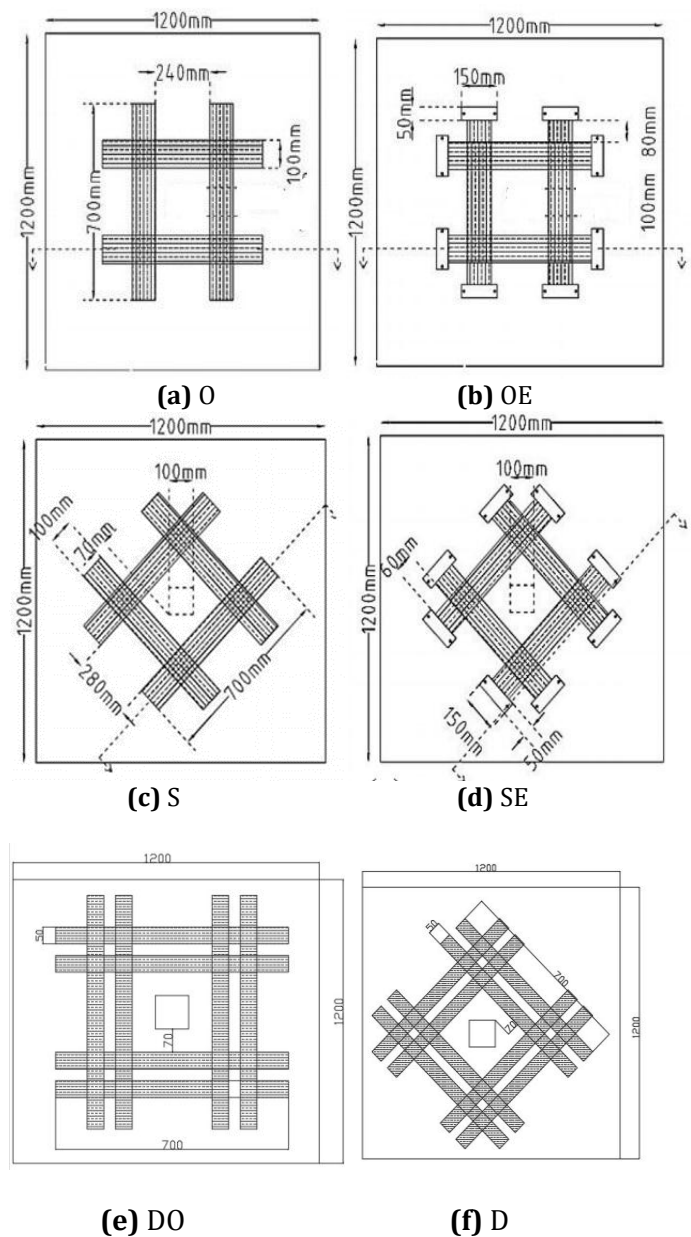


**Fig.11.** Diagram of strengthening schemes (a) O, (b) OE, (c) S, (d) SE, (e) DO, (f) DS

The mesh size and loading condition of other model same as the validated model. Such as the concrete element is C3D6R with 20 mm mesh size, the steel element also C3D6R with mesh size is 5mm, the epoxy element is COH3D6R, with mesh size 8mm, and the CFRP element is SC6R with mesh size 8mm. the interaction in these models same as in validated model such as the steel is embedded in concrete, epoxy tied in concrete, and the CFRP is pasted in epoxy. In order to reduce the computational time, one-quarter of the specimen was modelled. ie, the size concrete specimen is 600 x 600. The analysis is quasi static with velocity applied is 0 to 100mm/s in 0.3s with amplitude. so the deflection at

loading position move from 0 to 15 mm. this analysis gives the smooth load deflection curve.

### 5. RESULT AND DISCUSSION

In this project two section of analysis. First, simulate all strengthened flat slabs with CFRP and control specimen, for comparing the punching shear strength to the control specimen and each other strength. Second, simulate the high strength concrete and strengthened high concrete flat slabs for comparing punching strength of lower strength concrete and its strengthened flat slabs.

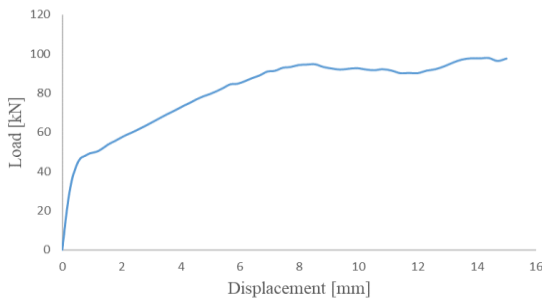


Fig. 12 Load Deflection Curve of control slab

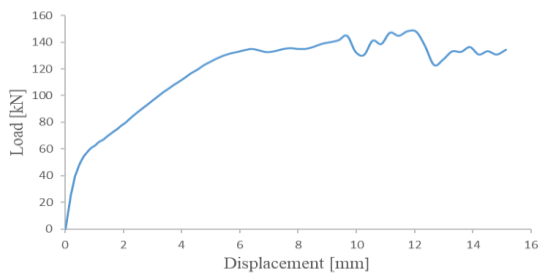


Fig. 13 Load Deflection Curve of specimen O

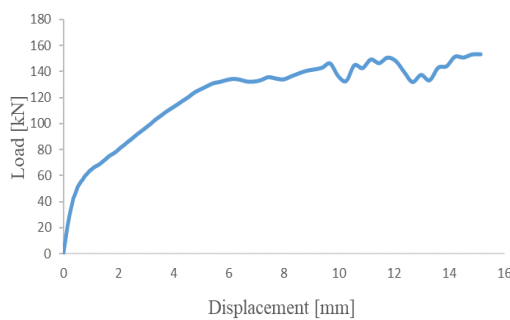


Fig. 14 Load Deflection Curve of specimen OE

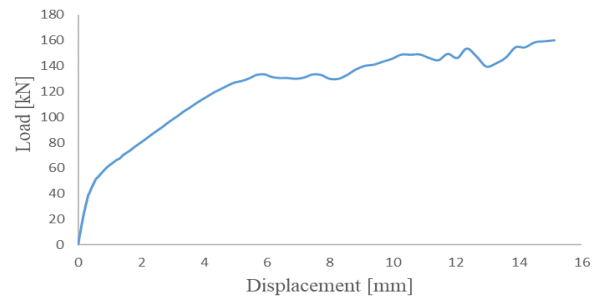


Fig. 15 Load Deflection Curve of specimen S

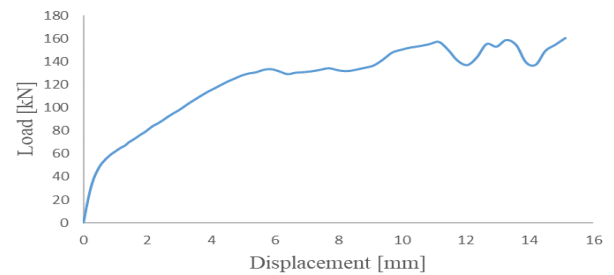


Fig. 16 Load Deflection Curve of specimen SE

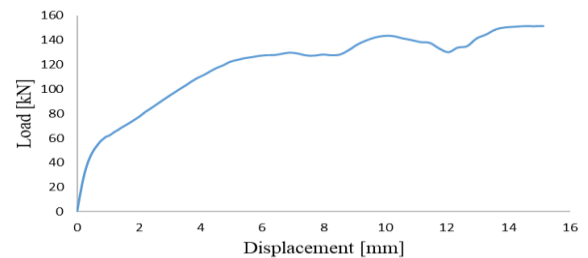


Fig. 17 Load Deflection Curve of specimen SE

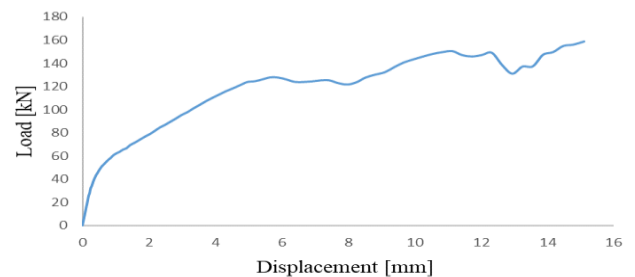


Fig. 18 Load Deflection Curve of specimen SE

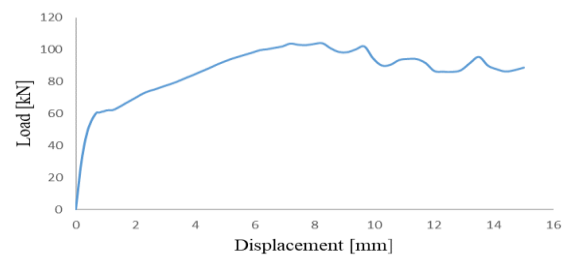


Fig. 19 Load Deflection Curve of 44MPa concrete flat slab

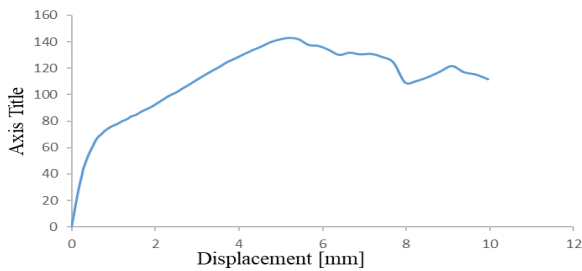


Fig.20 Load Deflection Curve of 44MPa strengthened concrete flat slab

### 5.1 Comparison of O, OE, S, & SE

Table-3 FE Modelling results of O, OE, S, & SE.

Specimen	Failure load (kN)	Displacement at failure(mm)
Control	94.6	8.53
O	144.73	9.67
OE	146.26	9.67
S	153.56	12.33
SE	156.73	11.14

The load deflection response of FE model in comparative study shows the variation of punching shear strength with respect to control specimen. It clearly shows that load is much more in external strengthening scheme compared to control specimen. The punching shear capacity of flat could be increased by installing strengthening scheme

A similar deflection increment behaviour was observed during the experiment from all tested specimens till they reach 40kN load (25% of the ultimate load). The specimens in which the CFRP strips were attached in skewed direction with end anchors had shown the lowest deflection increment rate with the highest load carrying capacity of 65% with respect to the control specimens. Further, the attaching of CFRP in skewed direction and the introduction of end anchorages onto the CFRP strips had caused for the reduction in deflection increment rate. This implies that the enhanced punching shear capacity was more than 53% to 65% during testing because the dominant failure mode was the flexural failure. The control specimen has lot of flexural cracks are developed in the analysis before punching shear failure.

The control specimen have more flexible crack before a sudden drop in its load-displacement relationship as seen in Fig 12 However, the strengthened specimens in series Fig. 13 to 16 failed in a brittle manner with a sudden drop in their load-displacement relationships

### 5.2 Comparison of O, S, DO & DS.

Table-4 FE Modelling results of O, S, DO & DS.

Specimen	Failure load (kN)	Displacement at failure(mm)
O	144.73	9.67
S	153.56	12.33
DO	143.324	10.25
DS	150.476	11.146

In this study the half amount of CFRP is specimen O&S is placed on DO&DS with interval 35mm in orthogonal and skewed direction, and its FE result of failure load less than its corresponding specimen ie., O&S. The space between the CFRP is influenced in the strength of the flat slab, the strength increment decreasing as well as the increasing space between the CFRP.

### 5.3 Comparison of strengthened 28MPa and 44MPa concrete flat slab specimen.

Table 5 FE Modelling results of high and lower strength of concrete flat slab.

Specimen	Failure load (kN)	Displacement at failure(mm)
Control(28MPa)	94.6	8.53
Control(44MPa)	104.14	8.25
O(28MPa)	144.73	9.67
O(44MPa)	144.84	5.43

The comparison of displacement at failure between different specimens made of 28 MPa and 44 MPa concrete strengths shows that punching shear strengthening by CFRP sheets is more effective for the slabs with higher strength concrete compared to those with lower strength. In 44MPa specimen the deflection decrease from 8.25 to 5.43. That is its post stiffness much more than the control specimens And the 28MPa have flexural failure is predominant.

By comparing the ultimate punching shear values of specimens 28MPa and 44MPa with its strengthening specimen the ultimate punching shear values increase by 52% and 40% respectively

## 6. CONCLUSIONS

The numerical studies were conducted to determine the performance of the external strengthening of slab-column connections with CFRP near the column face to enhance the punching shear performance. Total 9 numerical models are prepared, there is seven flat slab column specimens were strengthened externally with alternative CFRP arrangements

and another two specimens were kept as control samples. The following conclusions were made:

- The results indicated that the skewed placement of CFRP at the shear critical area is effective than that of orthogonal placement in the presence of end anchorage. More than 53% of punching shear capacity can be gained by the external strengthening of slab-column connections.
- Irrespective of the CFRP arrangement at the tension face of specimens, the provision of end anchorage to CFRP strips increases the load carrying capacity.
- Using CFRP sheet, in addition to steel reinforcing bars as flexural reinforcement improves the punching shear strength of slabs. This improvement can be significant for the slabs made of high strength concrete and low steel reinforcement ratio.
- The strengthened slabs exhibited much stiffer responses and lower deflections than the control slab.
- Same amount of CFRP pasted in flat slab as manner of half amount of single strip with particular spacing ( $d/2$ ) is significantly reduced the punching shear strength.

## REFERENCES

1. Al-Rifaie, Z. W. Guan, S. W. Jones (2017) "Quasi-Static Analysis of End Plate Beam-to-Column Connections" World Academy of Science, Engineering and Technology International Journal of Civil and Environmental Engineering Vol:11, No:7,936International.
2. ABAQUS 6.14
3. ACI Committee 318, (2008) "Building code requirements for structural concrete and commentary" ACI 318-08/ACI 318R-08, American Concrete Institute, Farmington Hills, MI.
4. Aikaterini S. Genikomsou Maria Anna Polak (2015) "Finite element analysis of punching shear of concrete slabs using damaged plasticity model in ABAQUS", Engineering Structures Vol.98 .pp.38–48
5. British Standards Institution Structural (1997) "use of concrete: Part 1 code of practice for design and construction", BS 8110. London, England.
6. Comité Euro-International du Béton, 1993. "CEB-FIB-model Code 1990: Design code". London: Thomas Telford
7. E.H. Rochdi, D. Bigaud, E. Ferrier, P. Hamelin (2004) "Ultimate behavior of CFRP strengthened RC flat slabs under a centrally applied load", Compos. Struct. 72 (1) (2006) 69–78,
8. K. Soudki, A.K. El-Sayed, T. Vanzwol (2012) "Strengthening of concrete slab-column connections using CFRP strips" J. King Saud Univ. – Eng. Sci. 24 (1) (2012) 25–33,
9. M.A.L. Silva, J.C.P.H. Gamage, S. Fawzia (2019), "Performance of slab-column connections of flat slabs strengthened with carbon fiber reinforced polymer" Case Studies in Construction Materials 11 e00275
10. Massimo Lapia, António Pinho Ramosb, Maurizio Orlandoa (2019) "Flat slab strengthening techniques against punching-shear" Engineering Structures Volume 180, Pages 160-180, Pages 160-180
11. M.L.V.P. Malalanayake, J.C.P.H. Gamage, M.A.L. Silva (2017) "experimental investigation on enhancing punching shear capacity of flat slabs using cfrp" 8th International Conference on Structural Engineering and Construction Management,
12. M.R. Esfahani, M.R. Kianoush, A.R. Moradi (2009), "Punching shear strength of interior slab-column connections strengthened with carbon fiber reinforced polymer sheets", Eng. Struct. 31 (7) 1535–1542.
13. Mostafiz Emtiaz , A.S.M. Alauddin Al Azad , H. M. Shahin and Sultan Al Shafian,(2017) "Numerical Analysis of a Reinforced Concrete Slab-Column Connection Subjected to Lateral & Vertical Loading" Proceedings of the International Multi Conference of Engineers and Computer Scientists 2017 Vol II,
14. R.H.M. Dissanayaka, M.A.L. Silva, L.P.G. Magallagoda, J.C.P.H. Gamage, (2018) "Physical behavior of CFRP retrofitted reinforced concrete slab-columnconnections" 9th International Conference on Sustainable Built Environment (ICSBE2018), Kandy, Sri Lanka, 2018.
15. Y. Tao<sup>1</sup> and J. F. Chen, M.ASCE 2 (2015) "Concrete Damage Plasticity Model for Modeling FRP-to-Concrete Bond Behavior" J. Compos. Constr., 2015, 19(1): 04014026
16. Yusuf Sümer, Muharrem Aktaş, (2015) "Defining parameters for concrete damage plasticity model" challenge journal of structural mechanics 1 (3) 149–155